Eur J Drug Metab Pharmacokinet (2018) 43:301–309
https://doi.org/10.1007/s13318-017-0450-x

ORIGINAL RESEARCH ARTICLE

# Identification of Uridine 5′-Diphosphate-Glucuronosyltransferases Responsible for the Glucuronidation of Mirabegron, a Potent and Selective $\beta_3$-Adrenoceptor Agonist, in Human Liver Microsomes

**Kentaro Konishi**[1] · **Daisuke Tenmizu**[1] · **Shin Takusagawa**[2]

Published online: 21 November 2017


**Abstract**

*Background and Objectives* Mirabegron is cleared by multiple mechanisms, including drug-metabolizing enzymes. One of the most important clearance pathways is direct glucuronidation. In humans, M11 (*O*-glucuronide), M13 (carbamoyl-glucuronide), and M14 (*N*-glucuronide) have been identified, of which M11 is one of the major metabolites in human plasma. The objective of this study was to identify the uridine 5′-diphosphate (UDP)-glucuronosyltransferase (UGT) isoform responsible for the direct glucuronidation of mirabegron using human liver microsomes (HLMs) and recombinant human UGTs (rhUGTs).

*Methods* Reaction mixtures contained 1–1000 μM mirabegron, 8 mM $MgCl_2$, alamethicin (25 μg/mL), 50 mM Tris–HCl buffer (pH 7.5), human liver microsome (HLM) or rhUGT (1.0 mg protein/mL), and 2 mM UDP-glucuronic acid in a total volume of 200 μL for 120 min at 37 °C. HLMs from 16 individuals were used for the correlation study, and mefenamic acid and propofol were used for the inhibition study.

*Results* Regarding M11 formation, rhUGT2B7 showed high activity among the rhUGTs tested (11.3 pmol/min/mg protein). This result was supported by the correlation between M11 formation activity and UGT2B7 marker enzyme activity (3-glucuronidation of morphine, $r^2 = 0.330$, $p = 0.020$) in individual HLMs; inhibition by mefenamic acid in pooled HLMs ($IC_{50} = 22.8$ μM); and relatively similar $K_m$ values between pooled HLMs and rhUGT2B7 (1260 vs. 486 μM). Regarding M13 and M14 formation, rhUGT1A3 and rhUGT1A8 showed high activity among the rhUGTs tested, respectively.

*Conclusions* UGT2B7 is the main catalyst of M11 formation in HLMs. Regarding M13 and M14 formation, UGT1A3 and UGT1A8 are strong candidates for glucuronidation, respectively.

**Key Points**

Mirabegron *O*-glucuronide, which is the main glucuronide among direct glucuronides, was formed mainly by UGT2B7.

UGT1A3 and UGT1A8 were the candidate isoforms which catalyzed the formation of mirabegron carbamoyl-glucuronide and *N*-glucuronide, respectively.

## 1 Introduction

Mirabegron [YM178, 2-(2-amino-1,3-thiazol-4-yl)-*N*-[4-(2-{[(2R)-2-hydroxy-2-phenylethyl]amino}ethyl)phenyl] acetamide] (Fig. 1) is a potent and selective agonist for the human $\beta_3$-adrenoceptor (AR) [1], and the first compound of a new pharmacological class for the treatment of overactive bladder (OAB) developed by Astellas Pharma Inc. (Tokyo, Japan). Mirabegron activates $\beta_3$-ARs on the detrusor muscle of the bladder to facilitate filling of the bladder and storage of urine without inhibiting bladder voiding

✉ Kentaro Konishi
kentaro.konishi@astellas.com

[1] Analysis and Pharmacokinetics Research Laboratories, Drug Discovery Research, Astellas Pharma Inc., 21, Miyukigaoka, Tsukuba-shi, Ibaraki 305-8585, Japan

[2] Clinical Pharmacology, Development, Astellas Pharma Inc., 2-5-1, Nihonbashi-Honcho, Chuo-ku, Tokyo 103-8411, Japan

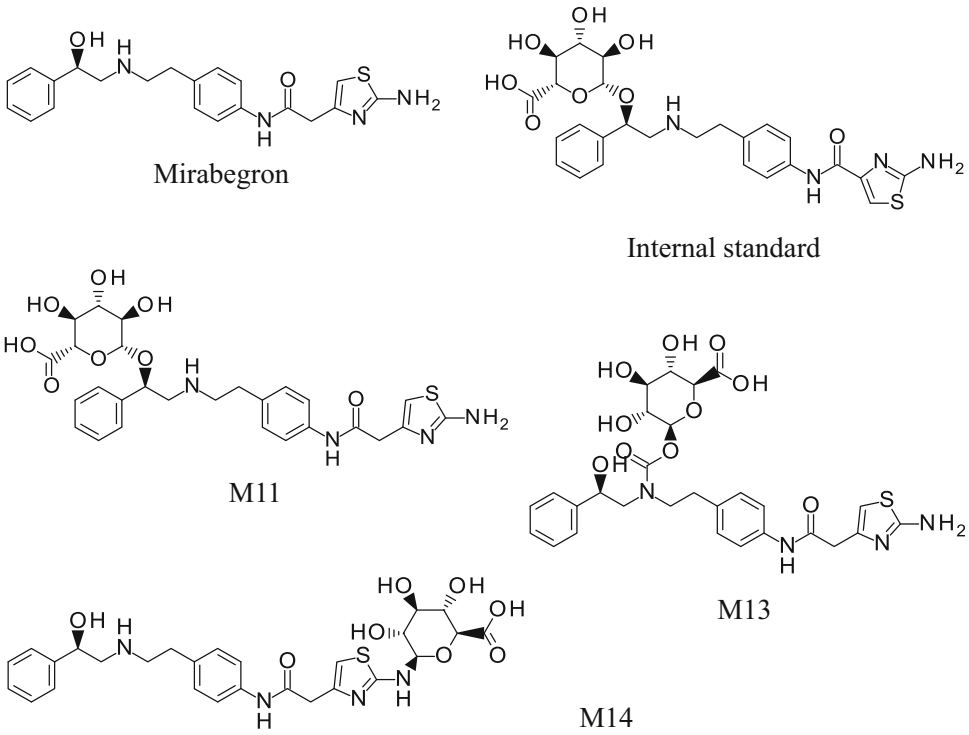


**Fig. 1** Chemical structures of mirabegron, M11, M13, M14, and internal standard

contractions [1, 2]. Pivotal phase 3 clinical trials confirmed that single daily oral administration of mirabegron at 25 and 50 mg is an effective treatment for OAB symptoms, with a low occurrence of side effects [3–6]. As of March 2017, mirabegron has been launched in about 50 countries, including Japan, the USA, Europe, and the Asia-Oceania region.

In humans receiving a single oral dose of [$^{14}$C]mirabegron (160 mg) as a solution, unchanged mirabegron was the most abundant component of radioactivity, accounting for about 22% of circulating radioactivity in plasma [7]. Of the administered radioactivity, 55% was excreted in urine as the unchanged form (approximately 25%) or metabolites (approximately 30%), and 34% was recovered in feces almost entirely as the unchanged form. More than half of the excreted radioactivity in urine was in metabolites, suggesting that metabolism plays a substantial role in mirabegron elimination. On the basis of the metabolites found in urine, major primary metabolic reactions of mirabegron in humans were estimated to be amide hydrolysis, followed by glucuronidation and *N*-dealkylation or oxidation of the secondary amine [7]. To date, butyrylcholinesterase (BChE), cytochrome P450 (CYP) 3A4, and CYP2D6 have been identified as responsible for the metabolism of mirabegron [8]. However, the uridine 5′-diphosphate (UDP)-glucuronosyltransferase (UGT) isoenzymes involved in the glucuronidation of mirabegron have not been determined.

In humans, three direct glucuronides, M11 (*O*-glucuronide of mirabegron), M13 (carbamoyl-glucuronide of mirabegron), and M14 (*N*-glucuronide of mirabegron) have been identified [7]. Of these, M11 was the most abundant metabolite in plasma and urine, and was identified as one of the major metabolites according to the International Conference on Harmonization of Technical Requirements for Registration of Pharmaceuticals for Human Use M3 (R2) guidance, since it represented 17% of total drug-related exposure in plasma in multiple-dose studies at oral doses of 25–100 mg daily. M13 and M14 were considered to be minor metabolites in humans, accounting for 1 and 6% of total drug-related exposure in plasma, respectively [9]. M11 and M13 were formed following both intravenous and oral administration, while M14 was observed only after oral administration [10], suggesting that M14 is mainly formed in the intestine.

In the present study, our primary objective was to identify the UGT isoform responsible for M11 formation in human liver using recombinant human UGTs (rhUGTs) and human liver microsomes (HLMs). Our secondary objective was to identify the isoforms responsible for M13 and M14 formation. Since direct glucuronidation is an important clearance pathway of mirabegron in humans, identification of the UGT isoform(s) for M11, M13, and M14 formation is indispensable for a comprehensive understanding of the overall metabolism of mirabegron.

## 2 Materials and Methods

### 2.1 Chemicals and Reagents

Mirabegron (YM178; Fig. 1), the *O*-glucuronide of mirabegron (M11, YM-382984; Fig. 1), the carbamoyl-glucuronide of mirabegron (M13, YM-538859; Fig. 1), the *N*-glucuronide of mirabegron (M14, YM-554028; Fig. 1) and internal standard for the determination of M11, M13, and M14 concentrations (YM-9674146; Fig. 1) were synthesized at Astellas Pharma Inc (Ibaraki, Japan). Pooled HLM (mixed gender, pool of $n = 50$) and a reaction phenotyping kit of HLMs from 16 individuals were purchased from XenoTech, LLC (Lenexa, KS, USA). rhUGTs (1A1, 1A3, 1A4, 1A6, 1A7, 1A8, 1A9, 1A10, 2B4, 2B7, 2B10, 2B15, and 2B17) expressed by baculovirus-infected insect cells were purchased from BD Biosciences (Woburn, MA, USA). UGT reaction mix solutions A and B were purchased from BD Biosciences. Mefenamic acid was purchased from Sigma-Aldrich (St. Louis, MO, USA). 2,6-Diisopropylphenol (propofol) was purchased from Kanto Chemical (Tokyo, Japan). Acetonitrile of high-performance liquid chromatography (HPLC) grade was purchased from Wako Pure Chemical Industries (Osaka, Japan). Methanol of HPLC grade was purchased from Nacalai Tesque (Kyoto, Japan). Purified water was prepared using a Milli-Q water purification system from Merck Millipore (Billerica, MA, USA). All other chemicals, including dimethyl sulfoxide (DMSO), were of the appropriate purity commercially available.

### 2.2 In Vitro Assay of Mirabegron Glucuronidation

Incubations for mirabegron glucuronidation by HLMs and rhUGTs were conducted as described below. Protein concentration and incubation time were 1.0 mg protein/mL and 120 min, respectively. Typical incubation mixtures contained 1–1000 μM mirabegron for kinetic studies, 8 mM $MgCl_2$, alamethicin (25 μg/mL), 50 mM Tris–HCl buffer (pH 7.5), enzyme preparation (HLM or rhUGT), and 2 mM UDP-glucuronic acid (UDPGA) in a total volume of 200 μL. It is known that HLM and rhUGTs are fully activated by the addition of alamethicin [11]. Mirabegron was dissolved in DMSO to prepare a 200 mM mirabegron solution and the solution was diluted with DMSO to prepare the various concentrations. An aliquot of 1 μL mirabegron solution was added to the incubation mixture. After the incubation mixture without UDPGA was allowed to stand on ice, the mixture was preincubated for 10 min at 37 °C, and then the reaction was started by adding UDPGA. After incubation for 120 min, the reaction was terminated by precipitating proteins via the addition of 2 mL of *tert*-butylmethylether. The samples were centrifuged for 15 min at 5 °C (1870×*g*). The upper layer (mainly *tert*-butylmethylether) was removed and an aliquot (100 μL) of the lower layer was added to 40 μL of an internal standard solution (1 μg/mL). After filtration using a membrane filter, 5 μL of the filtrate was injected into the liquid chromatography–tandem mass spectrometry (LC–MS/MS) system.

### 2.3 Correlation Analysis for Individual HLMs

M11 formation activity was measured in HLMs prepared from 16 individual human livers. The activity of each UGT isoform in each HLM determined by isoform-specific reaction markers (UGT1A1, 3-glucuronidation of 17β-estradiol; UGT1A4, glucuronidation of trifluoperazine; UGT1A9, glucuronidation of propofol; UGT2B7, 3-glucuronidation of morphine) was provided by XenoTech, LLC. Although morphine is known not to be a selective substrate of UGT2B7, we considered it reasonable to support the contribution of UGT2B7 because morphine 3-glucuronide is known to be mainly formed by UGT2B7 [12, 13]. The assays were performed as described in the Sect. 2.2 with 100 μM mirabegron. Correlation between M11 formation activity and each isoform-specific reaction marker activity was determined by correlation analysis using GraphPad Prism version 5 (GraphPad Software Inc., San Diego, CA, USA). Correlation coefficient ($r$) was calculated by Pearson test and a $p$ value of less than 0.05 was considered to be statistically significant.

### 2.4 Effects of Typical UGT Inhibitors on Mirabegron Glucuronidation in Pooled HLM

For UGT inhibitors, mefenamic acid and propofol were selected. Although these are not selective inhibitors of UGT2B7 and UGT1A9, respectively [14–20], they were used to obtain supportive data. The assay procedure is described in the Sect. 2.2 with 100 μM mirabegron and mefenamic acid (0–100 μM) or propofol (0–100 μM). The concentration range of inhibitors was set as sufficient to inhibit at least UGT2B7 or UGT1A9, respectively, from the previous literature described above. The percentages of glucuronidation rate relative to the vehicle control and $IC_{50}$ values were calculated.

### 2.5 LC–MS/MS Analysis for Assessment of M11, M13, and M14 Formation

For the calibration curve, M11, M13, and M14 were dissolved in 50% methanol, DMSO, and methanol, respectively, to prepare 1 mg/mL solutions and the solutions were diluted with 50% methanol to prepare the various concentrations. The concentrations of M11, M13, and M14 were determined according to a previous report with minor

modifications [21]. Briefly, an LC–MS/MS system composed of an LC-20AD series HPLC (Shimadzu, Kyoto, Japan) coupled with a triple quadrupole mass spectrometer using multiple reaction monitoring in positive electrospray ionization mode (4000QTRAP; AB Sciex, Foster City, CA, USA) was used. A Synergi Fusion-RP (2.0 × 150 mm column with 4 μm particle size; Phenomenex, Inc., Torrance, CA, USA) connected to a SecurityGuard Standard, Fusion-RP (4 × 2.0 mm guard column; Phenomenex, Inc.) was used. Mobile phase A consisted of a 75 mM ammonium acetate solution, 0.15% formic acid, and purified water (1:1:8, v/v/v) and mobile phase B was acetonitrile. The temperature of the column was kept at 40 °C and the flow rate was 0.5 mL/min. The gradient program was set as 0.00 min (B: 20%) to 4.00 min (B: 40%) in linear mode, and 4.01 min to 5.00 min was set as isocratic (B: 20%). The monitoring ions selected were *m/z* 573.1–146.1 for M11, *m/z* 617.1–113.0 for M13, *m/z* 573.1–146.1 for M14, and *m/z* 559.1–246.0 for IS. Retention time of M11, M13, M14, and internal standard was about 1.8, 2.7, 1.3, and 2.5 min, respectively. Quantitation of the analytes was performed using Analyst version 1.5 (AB Sciex).

### 2.6 Kinetic Analyses for M11, M13, and M14 Formation

Microsoft Excel 2007 for Windows (Microsoft Corporation, Redmond, WA, USA) was used to calculate M11, M13, or M14 formation activity. The equation is described as below:

$$\text{M}x\text{ formation activity} = \frac{[\text{M}x]}{\text{MW} \times \text{RT} \times [\text{P}]} \times 1000$$

where M*x* is M11, M13 or M14 formation activity in pmol/min/mg protein, [M*x*] is M11, M13 or M14 concentration in ng/mL, MW is the molecular weight of free form of M11, M13 or M14, RT is the reaction time in min, [P] is the final protein concentration in reaction mixtures in mg protein/mL.

The enzyme kinetic parameters (Michaelis–Menten constant $K_m$ and maximum velocity $V_{max}$) were determined by fitting the data to the Michaelis–Menten equation (Eq. 1) according to a nonlinear least-squares regression analysis using WinNonlin version 6.1 (Pharsight Corp.; Mountain View, CA, USA) [22]:

$$V = V_{max} \times [S]/(K_m + [S]), \quad (1)$$

where $V$ is formation activity and $[S]$ is substrate concentration.

The value of intrinsic clearance ($CL_{int}$) was calculated using Microsoft Excel 2007 for Windows (Microsoft Corporation) using the following equation:

$$CL_{int} = V_{max}/K_m. \quad (2)$$

The residual activity (% of control) of M11 formation was calculated using Microsoft Excel 2007 for Windows (Microsoft Corporation). The equation is described below:

Residual activity of M11 formation (%)
= M11 formation activity at each inhibitor concentration/
M11 formation activity in control samples × 100.

The values of inhibitor concentration showing the half formation activity ($IC_{50}$) were determined by fitting of the relationship between the residual activity and the inhibitor concentration using WinNonlin version 6.1 (Pharsight Corp.) using Eq. (3). When the $IC_{50}$ value was not calculated because of high residual activity at all concentrations of inhibitor or above the highest concentration tested, the result was expressed as "$IC_{50}$ > the maximum concentration of the inhibitor":

$$E = E_{min} + (E_{max} - E_{min})/\{1 + ([I]/IC_{50})^n\}, \quad (3)$$

where $E$ is the residual activity, $E_{max}$ is maximum of residual activity, $E_{min}$ is minimum of residual activity, $I$ is inhibitor concentration, and n is the Hill coefficient.

## 3 Results

### 3.1 M11, M13, and M14 Formation in rhUGTs

UGT1A9 and UGT2B7 showed the highest activity for M11 formation (13.4 and 11.3 pmol/min/mg protein, respectively), followed by UGT1A4, 1A8, 1A1, 2B4, 2B17, 1A3, 1A7, and 1A6 (Fig. 2a). No other UGT isoform (UGT1A10, 2B10, or 2B15) showed M11 formation activity. Regarding M13 formation, UGT1A3 and UGT1A9 showed the highest activity (4.03 and 0.220 pmol/min/mg protein, respectively), followed by UGT1A1, 1A7, 2B15, 1A8, and 2B7 (Fig. 2b). No other UGT isoform (UGT1A4, 1A6, 1A10, 2B4, 2B10, and 2B17) showed M13 formation activity. M14 formation was catalyzed mainly by UGT1A8, 1A10, and 1A9 (0.576, 0.184, and 0.177 pmol/min/mg protein, respectively) followed by UGT1A1, 1A3, 1A4, 1A7, and 2B7 (Fig. 2c). No other UGT isoform (UGT1A6, 2B4, 2B10, 2B15, and 2B17) showed M14 formation activity.

### 3.2 Correlation Analyses for M11 Formation Using Individual HLMs

A significant correlation was observed between M11 formation activity and the marker enzyme activities for UGT2B7 ($r^2 = 0.330$, $p = 0.020$; Fig. 3a) and UGT1A4 ($r^2 = 0.649$, $p = 0.0002$; Fig. 3b), although there was no correlation between M11 formation activity and that for

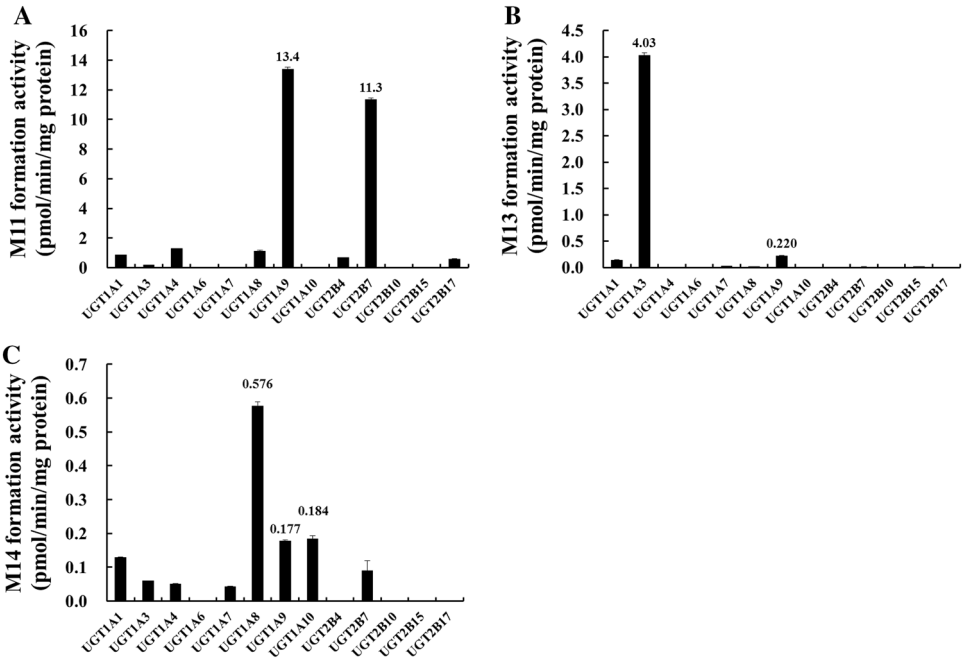


**Fig. 2** M11, M13, and M14 formation activities in rhUGTs. **a–c** M11, M13, and M14 formation activities in each rhUGT, respectively. Each rhUGT (1 mg protein/mL) was incubated with 100 μM mirabegron and 2 mM UDPGA at 37 °C for 120 min. Mean and SD of triplicate samples are represented. *UGT* uridine 5′-diphosphate-glucuronosyltransferase

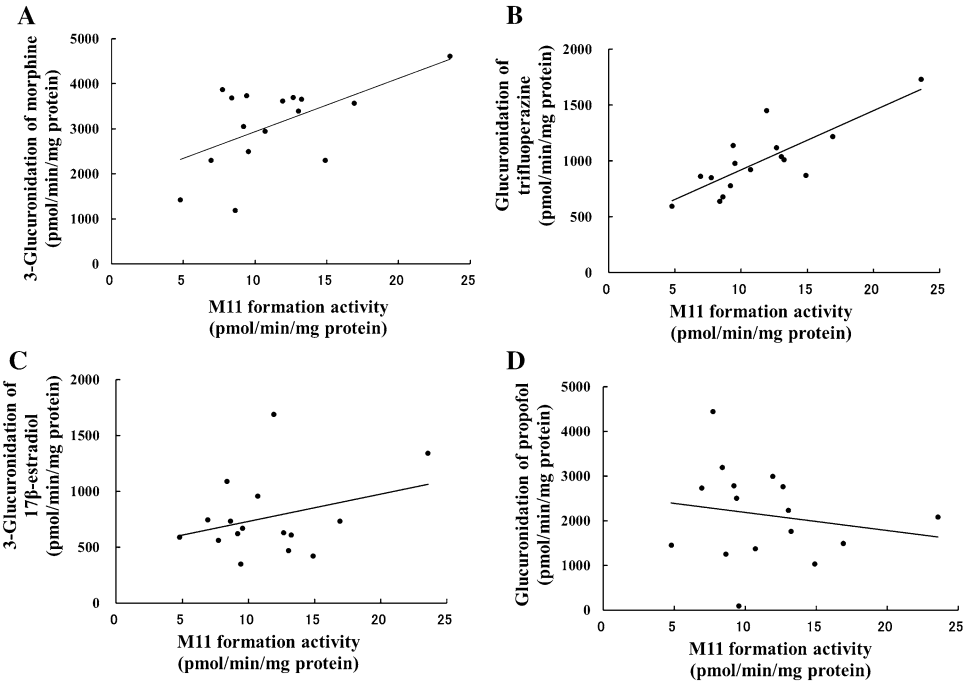


**Fig. 3** Correlation between M11 formation activity and respective UGT marker enzyme activity in HLMs from 16 individual human livers. **a–d** The correlation between M11 formation activity and UGT2B7, UGT1A4, UGT1A1, and UGT1A9 marker enzyme activity, respectively. Individual HLMs (1 mg protein/mL) were incubated with 100 μM mirabegron and 2 mM UDPGA at 37 °C for 120 min. UGT marker enzyme activities were provided by the supplier. Data represent the mean of triplicate samples and lines are from linear regression analysis

UGT1A1 ($r^2 = 0.099$, $p = 0.235$; Fig. 3c) and UGT1A9 ($r^2 = 0.031$, $p = 0.511$; Fig. 3d).

### 3.3 Effects of Typical UGT Inhibitors on M11 Formation in Pooled HLM

M11 formation in pooled HLM was inhibited by mefenamic acid and the $IC_{50}$ value was estimated to be $22.8 \pm 6.0$ μM (Fig. 4a). On the other hand, propofol did not clearly inhibit M11 formation even at the maximum concentration of 100 μM and the $IC_{50}$ value was estimated to be > 100 μM (Fig. 4b).

### 3.4 Kinetics of M11 Formation in Pooled HLM and rhUGT2B7

M11 formation activities in pooled HLM were fitted to the Michaelis–Menten equation shown in Fig. 5a. $K_m$ values

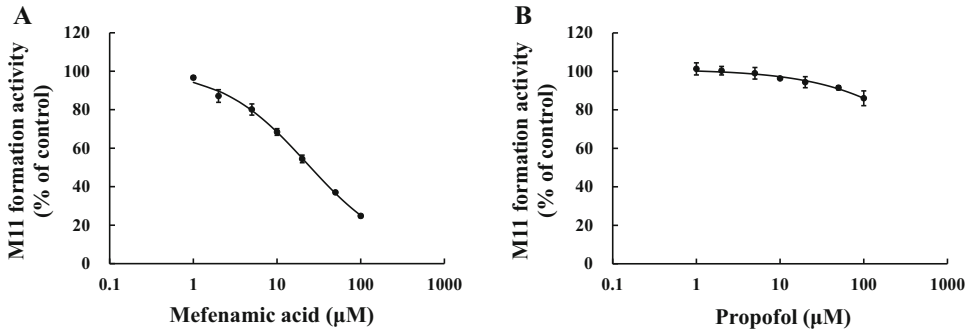


**Fig. 4** Effect of UGT inhibitors on M11 formations in pooled HLM. Pooled HLM (1 mg protein/mL) was incubated with 100 μM mirabegron, UGT inhibitor (**a** mefenamic acid, **b** propofol), and 2 mM UDPGA at 37 °C for 120 min. Formation activity of each (% of control) represents mean and SD of triplicate samples

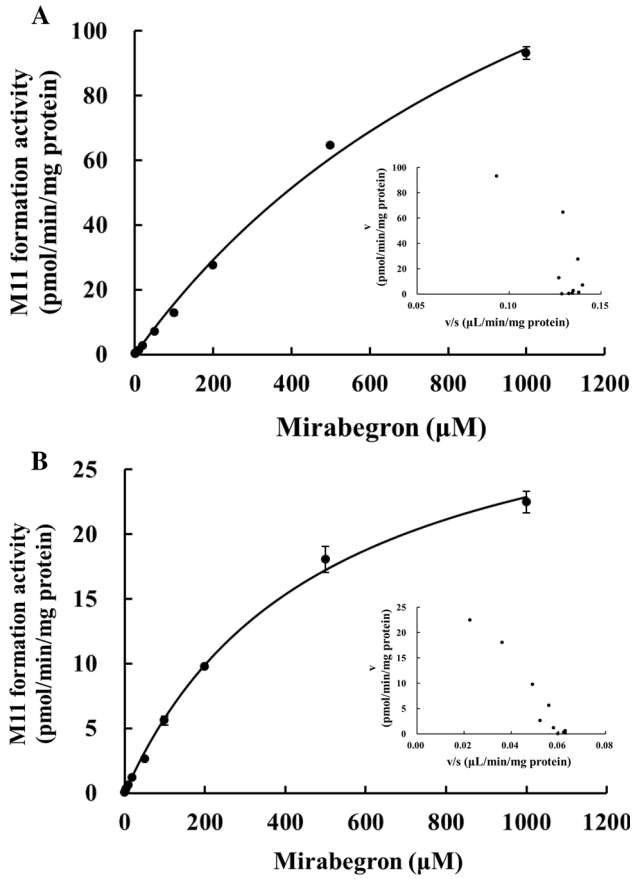


**Fig. 5** M11 formation by pooled HLM and rhUGT2B7. Michaelis–Menten plots (**a** for pooled HLM and **b** for rhUGT2B7) and Eadie–Hofstee plots (inset figures) are shown. Pooled HLM or rhUGT2B7 (1 mg protein/mL) was incubated with 1–1000 μM mirabegron and 2 mM UDPGA at 37 °C for 120 min. Mean and SD of triplicate samples are represented in Michaelis–Menten plots and mean of triplicate samples are represented in Eadie–Hofstee plots. *UGT* uridine 5′-diphosphate-glucuronosyltransferase, *v* formation activity, *s* substrate concentration

for M11 formation were estimated as $>1000$ ($1260 \pm 205$) μM (values in parentheses are extrapolated values). The extrapolated $V_{max}$ and calculated $CL_{int}$ values for M11 formation were $214 \pm 22$ pmol/min/mg protein and 0.169 μL/min/mg protein, respectively. On the other hand, M11 formation activities in rhUGT2B7 were also fitted to Michaelis–Menten equation shown in Fig. 5b. $K_m$ values for M11 formation were estimated as $486 \pm 40$ μM. The calculated $V_{max}$ and $CL_{int}$ values for M11 formation were $34.0 \pm 1.3$ pmol/min/mg protein and 0.070 μL/min/mg protein, respectively.

## 4 Discussion and Conclusion

We conducted several in vitro studies to identify the UGT isoforms responsible for the metabolism of mirabegron in human liver. Several studies were required because it is generally difficult to draw conclusions from a single study, due to the limited information about selective UGT substrates/inhibitors and the expression level differences of each isoform in human liver. Among in vitro studies, the use of rhUGTs is considered most reliable for the identification of UGT isoforms, as it is described in the draft guidance for industry published from the US Food and Drug Administration (FDA) (CDER, 2012). In the present study, therefore, we placed the greatest emphasis on the results of studies using rhUGTs.

The results of study using rhUGTs suggested that various UGT isoforms were involved in mirabegron glucuronidation (Fig. 2). Regarding M11 formation, UGT1A9 and UGT2B7 showed the highest activity among the rhUGTs tested, whereas M11 formation activities via UGT1A1 and UGT1A4 were negligible. A correlation study using individual HLMs indicated the involvement of UGT2B7, whereas the involvement of UGT1A1 and UGT1A9 was non-significant (Fig. 3). Mefenamic acid has inhibitory effects on UGT2B7, UGT1A1, and/or UGT1A9, and the results of the inhibition study using mefenamic acid suggested the involvement of these UGT isoforms (Fig. 4a). The involvement of UGT1A1 and UGT1A9 was, however,

**Table 1** Summary of the study results for M11 formation

| M11 formation | UGT1A1 | UGT1A4 | UGT1A9 | UGT2B7 |
|---|---|---|---|---|
| rhUGTs study | Negative | Negative | Positive | Positive |
| Correlation study | Negative | Positive | Negative | Positive |
| Inhibition study | Positive | ND | Negative | Positive |
| Kinetics study | ND | ND | ND | Positive |

Positive: possibility of contribution to M11 formation, negative: less possibility of contribution to M11 formation, ND no data

denied, for the following reasons: (1) the study using rUGT1A1 suggested that the contribution of UGT1A1 was low (Fig. 2a), and no correlation was seen between M11 formation and 17β-estradiol 3-glucuronidation activities in individual HLMs (Fig. 3a); (2) no correlation was observed between M11 formation and propofol glucuronidation activities in individual HLMs (Fig. 3c), and propofol did not inhibit M11 formation in HLMs at a concentration up to 100 μM (Fig. 4b). Propofol was reported to inhibit not only UGT1A9 but also UGT2B7. However, the $IC_{50}$ value for UGT1A9 inhibition (approximately 50–100 μM) was lower than that for UGT2B7 inhibition (over 400 μM) [18, 20]. The finding that propofol at a concentration up to 100 μM did not inhibit the M11 formation supported the idea that M11 formation in HLMs was mainly via UGT2B7, and not UGT1A9. Furthermore, $K_m$ values for M11 formation in pooled HLM and rhUGT2B7 were relatively similar (1260 [extrapolation value] vs. 486 μM, respectively) (Fig. 5). Taken together, these results indicate that the main contributor to M11 formation in humans is UGT2B7, whereas the contribution of UGT1A1 and UGT1A9 seems to be low (Table 1).

In the correlation studies, a significant correlation was observed between M11 formation activity and the marker activity of UGT1A4 in individual HLMs (Fig. 3b). However, rhUGT1A4 did not show a significant activity for M11 formation (Fig. 2a). Although no clear reason has been identified, one possibility for this discrepancy may reflect inter-correlation between UGT1A4 and 2B7 activities in individual HLMs, which were used for the correlation experiment ($r = 0.683$; data provided by XenoTech). Considering the possibility and the results of study using rUGT1A4, the correlation observed for UGT1A4 was considered to be an artifact or coincidence, and the contribution of UGT1A4 to M11 formation in humans was judged to be low.

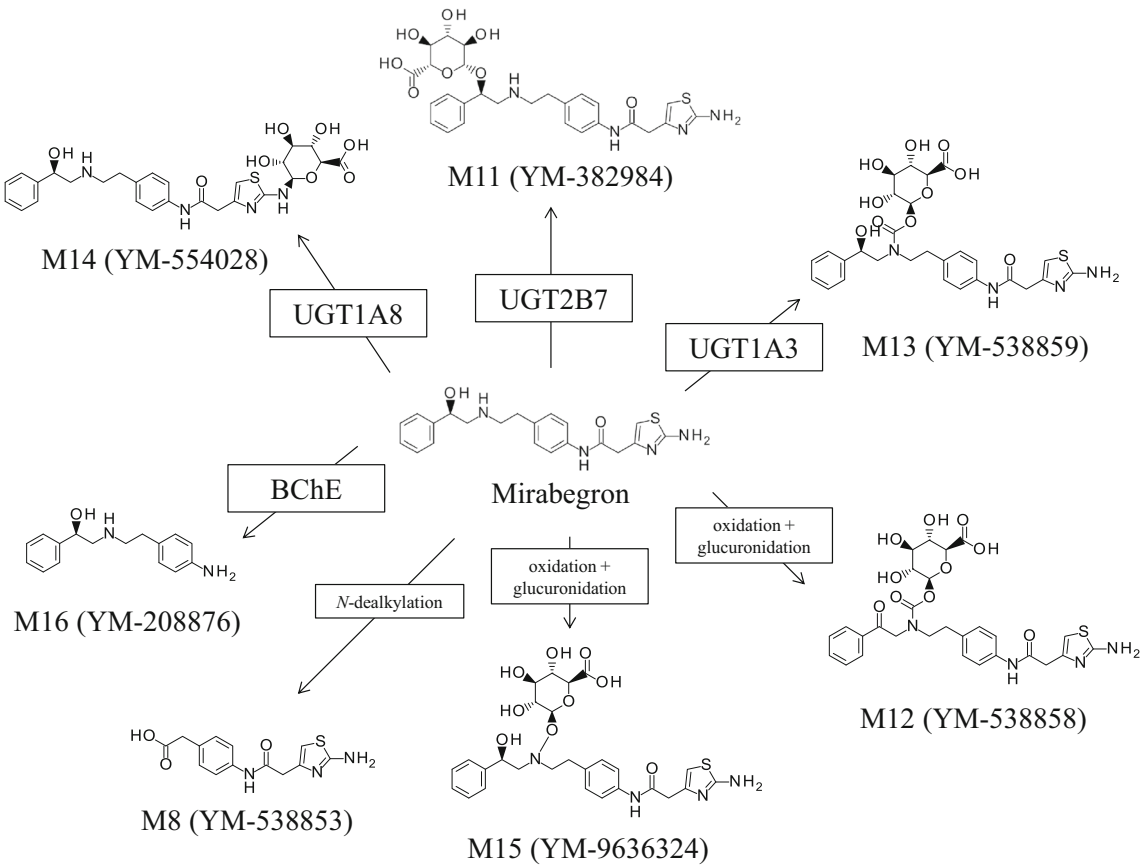


**Fig. 6** Overall metabolic pathways of mirabegron. *UGT* uridine 5′-diphosphate-glucuronosyltransferase, *BChE* butyrylcholinesterase

It was reported that fatty acids were released during the incubation and influenced an increase in the $K_m$ value regarding UGT2B7 substrates [23]. Although bovine serum albumin, which binds to fatty acids, was not added in the incubation buffer in the study, rhUGT2B7 activity was shown to be high (Fig. 2), meaning that even under the condition that the reaction via UGT2B7 was somewhat inhibited, the UGT2B7 contribution to M11 formation was supported. In addition, considering that steady-state maximum mirabegron plasma concentration following multiple 50 mg doses (approximately 50 ng/mL; 0.125 μM) [9], is far from the $K_m$ value, M11 formation activity may not saturate in clinical settings.

For M13 and M14 formation, the results of studies using rhUGTs suggested that UGT1A3 and UGT1A8 were responsible in humans, respectively (Fig. 2b, c). As described in Sect. 1, M11 and M13 were formed following both intravenous and oral administration, while M14 was observed only after oral administration [10]. From this observation, M14 appears to be formed mainly in the human intestine, rather than in the human liver. Indeed, in studies using rhUGTs, M14 formation was suggested to be catalyzed by UGT1A8, which is known to be predominantly expressed in human intestine [24, 25].

It is known that there are genetic polymorphisms in UGT2B7, namely UGT2B7*1 and UGT2B7*2. The frequencies of the UGT2B7*1 and UGT2B7*2 alleles are 0.511 and 0.489 in Caucasians and 0.732 and 0.268 in Japanese, respectively. Regarding UGT2B7 activity, statistically significant differences were not observed between UGT2B7*1 and UGT2B7*2 [26]. Taken together the information that mirabegron is cleared by multiple pathways, including renal and possibly biliary excretion and metabolism (BChE, CYP3A4, CYP2D6 and UGTs) [8], polymorphism of UGT2B7 is unlikely to have a significant effect on mirabegron pharmacokinetics. Multiple pathway elimination can also be regarded as an advantage from the viewpoint of drug–drug interaction (DDI). It was reported that fluconazole, a known UGT2B7 inhibitor, increased the exposure of zidovudine, a typical UGT2B7 substrate, to 1.74-fold [27]. Because drugs with a metabolic pathway restricted to one enzyme generally have a much larger fold inhibition when the enzyme is inhibited, the magnitude of DDI between mirabegron and UGT2B7 inhibitors might not be severe compared to that of zidovudine.

In summary, this study showed that catalysis of M11 formation in human liver was mainly by UGT2B7. Regarding M13 and M14 formation, results using rhUGTs indicated that UGT1A3 and UGT1A8 were candidate UGT isoforms. Considering these findings together with previous findings for the involvement of BChE, CYP3A4 and CYP2D6 in mirabegron metabolism, we have now clarified the overall metabolic pathways of mirabegron (Fig. 6). This study will aid the understanding of mirabegron disposition and safety in humans.

**Acknowledgements** The authors would like to sincerely thank Mr. Tadashi Hashimoto, Dr. Kiyoshi Noguchi, and Dr. Takashi Usui for their useful suggestions about the experiments and Dr. Toshifumi Shiraga, Dr. Tsuyoshi Minematsu, Dr. Yasuhisa Nagasaka, Dr. Takafumi Iwatsubo, Dr. Yoichi Naritomi, Mr. Aiji Miyashita, and Dr. Kenji Tabata for their contribution to this study.

**Author Contributions** *Participated in research design* Mr. Kentaro Konishi, Dr. Daisuke Tenmizu, and Dr. Shin Takusagawa. *Conducted experiments* Mr. Kentaro Konishi. *Performed data analysis* Mr. Kentaro Konishi, Dr. Daisuke Tenmizu, and Dr. Shin Takusagawa. *Wrote or contributed to the writing of the manuscript* Mr. Kentaro Konishi, Dr. Daisuke Tenmizu, and Dr. Shin Takusagawa

**Compliance with Ethical Standards**

**Conflict of interest** Mr. Kentaro Konishi, Dr. Daisuke Tenmizu and Dr. Shin Takusagawa are employees of Astellas Pharma, Japan.

**Funding** This study was sponsored by Astellas Pharma, Japan. Editorial support was funded by Astellas Pharma, Japan.

## References

1. Takasu T, Ukai M, Sato S, Matsui T, Nagase I, Maruyama T, et al. Effect of (R)-2-(2-aminothiazol-4-yl)-4′-{2-[(2-hydroxy-2-phenylethyl)amino]ethyl} acetanilide (YM178), a novel selective beta3-adrenoceptor agonist, on bladder function. J Pharmacol Exp Ther. 2007;321(2):642–7. https://doi.org/10.1124/jpet.106.115840.
2. Yamaguchi O, Chapple CR. Beta3-adrenoceptors in urinary bladder. Neurourol Urodyn. 2007;26(6):752–6. https://doi.org/10.1002/nau.20420.
3. Herschorn S, Barkin J, Castro-Diaz D, Frankel JM, Espuna-Pons M, Gousse AE, et al. A phase III, randomized, double-blind, parallel-group, placebo-controlled, multicentre study to assess the efficacy and safety of the beta(3) adrenoceptor agonist, mirabegron, in patients with symptoms of overactive bladder. Urology. 2013;82(2):313–20. https://doi.org/10.1016/j.urology.2013.02.077.
4. Khullar V, Amarenco G, Angulo JC, Cambronero J, Hoye K, Milsom I, et al. Efficacy and tolerability of mirabegron, a beta(3)-adrenoceptor agonist, in patients with overactive bladder: results from a randomised European–Australian phase 3 trial. Eur Urol. 2013;63(2):283–95. https://doi.org/10.1016/j.eururo.2012.10.016.
5. Nitti VW, Khullar V, van Kerrebroeck P, Herschorn S, Cambronero J, Angulo JC, et al. Mirabegron for the treatment of overactive bladder: a prespecified pooled efficacy analysis and pooled safety analysis of three randomised, double-blind, placebo-controlled, phase III studies. Int J Clin Pract. 2013;67(7):619–32. https://doi.org/10.1111/ijcp.12194.
6. Yamaguchi O, Marui E, Kakizaki H, Homma Y, Igawa Y, Takeda M, et al. Phase III, randomised, double-blind, placebo-controlled study of the beta3-adrenoceptor agonist mirabegron, 50 mg once daily, in Japanese patients with overactive bladder. BJU Int. 2014;113(6):951–60. https://doi.org/10.1111/bju.12649.
7. Takusagawa S, van Lier JJ, Suzuki K, Nagata M, Meijer J, Krauwinkel W, et al. Absorption, metabolism and excretion of [(14)C]mirabegron (YM178), a potent and selective beta(3)-

adrenoceptor agonist, after oral administration to healthy male volunteers. Drug Metab Dispos. 2012;40(4):815–24. https://doi.org/10.1124/dmd.111.043588.
8. Takusagawa S, Yajima K, Miyashita A, Uehara S, Iwatsubo T, Usui T. Identification of human cytochrome P450 isoforms and esterases involved in the metabolism of mirabegron, a potent and selective beta3-adrenoceptor agonist. Xenobiotica. 2012;42(10):957–67. https://doi.org/10.3109/00498254.2012.675095.
9. Krauwinkel W, van Dijk J, Schaddelee M, Eltink C, Meijer J, Strabach G, et al. Pharmacokinetic properties of mirabegron, a beta3-adrenoceptor agonist: results from two phase I, randomized, multiple-dose studies in healthy young and elderly men and women. Clin Ther. 2012;34(10):2144–60. https://doi.org/10.1016/j.clinthera.2012.09.010.
10. Eltink C, Lee J, Schaddelee M, Zhang W, Kerbusch V, Meijer J, et al. Single dose pharmacokinetics and absolute bioavailability of mirabegron, a beta(3)-adrenoceptor agonist for treatment of overactive bladder. Int J Clin Pharmacol Ther. 2012;50(11):838–50. https://doi.org/10.5414/CP201782.
11. Fisher MB, Campanale K, Ackermann BL, VandenBranden M, Wrighton SA. In vitro glucuronidation using human liver microsomes and the pore-forming peptide alamethicin. Drug Metab Dispos. 2000;28(5):560–6.
12. Coffman BL, Rios GR, King CD, Tephly TR. Human UGT2B7 catalyzes morphine glucuronidation. Drug Metab Dispos. 1997;25(1):1–4.
13. Ohno S, Kawana K, Nakajin S. Contribution of UDP-glucuronosyltransferase 1A1 and 1A8 to morphine-6-glucuronidation and its kinetic properties. Drug Metab Dispos. 2008;36(4):688–94. https://doi.org/10.1124/dmd.107.019281.
14. Joo J, Kim YW, Wu Z, Shin JH, Lee B, Shon JC, et al. Screening of non-steroidal anti-inflammatory drugs for inhibitory effects on the activities of six UDP-glucuronosyltransferases (UGT1A1, 1A3, 1A4, 1A6, 1A9 and 2B7) using LC–MS/MS. Biopharm Drug Dispos. 2015;36(4):258–64. https://doi.org/10.1002/bdd.1933.
15. Mano Y, Usui T, Kamimura H. Inhibitory potential of nonsteroidal anti-inflammatory drugs on UDP-glucuronosyltransferase 2B7 in human liver microsomes. Eur J Clin Pharmacol. 2007;63(2):211–6. https://doi.org/10.1007/s00228-006-0241-9.
16. Mano Y, Usui T, Kamimura H. Predominant contribution of UDP-glucuronosyltransferase 2B7 in the glucuronidation of racemic flurbiprofen in the human liver. Drug Metab Dispos. 2007;35(7):1182–7. https://doi.org/10.1124/dmd.107.015347.
17. Mano Y, Usui T, Kamimura H. The UDP-glucuronosyltransferase 2B7 isozyme is responsible for gemfibrozil glucuronidation in the human liver. Drug Metab Dispos. 2007;35(11):2040–4. https://doi.org/10.1124/dmd.107.017269.
18. Mano Y, Usui T, Kamimura H. Contribution of UDP-glucuronosyltransferases 1A9 and 2B7 to the glucuronidation of indomethacin in the human liver. Eur J Clin Pharmacol. 2007;63(3):289–96. https://doi.org/10.1007/s00228-007-0261-0.
19. Walsky RL, Bauman JN, Bourcier K, Giddens G, Lapham K, Negahban A, et al. Optimized assays for human UDP-glucuronosyltransferase (UGT) activities: altered alamethicin concentration and utility to screen for UGT inhibitors. Drug Metab Dispos. 2012;40(5):1051–65. https://doi.org/10.1124/dmd.111.043117.
20. Zhang D, Chando TJ, Everett DW, Patten CJ, Dehal SS, Humphreys WG. In vitro inhibition of UDP glucuronosyltransferases by atazanavir and other HIV protease inhibitors and the relationship of this property to in vivo bilirubin glucuronidation. Drug Metab Dispos. 2005;33(11):1729–39. https://doi.org/10.1124/dmd.105.005447.
21. Teijlingen R, Meijer J, Takusagawa S, Gelderen M, Beld C, Usui T. Development and validation of LC–MS/MS methods for the determination of mirabegron and its metabolites in human plasma and their application to a clinical pharmacokinetic study. J Chromatogr B Analyt Technol Biomed Life Sci. 2012;887–888:102–11. https://doi.org/10.1016/j.jchromb.2012.01.018.
22. Houston JB, Kenworthy KE. In vitro-in vivo scaling of CYP kinetic data not consistent with the classical Michaelis–Menten model. Drug Metab Dispos. 2000;28(3):246–54.
23. Rowland A, Gaganis P, Elliot DJ, Mackenzie PI, Knights KM, Miners JO. Binding of inhibitory fatty acids is responsible for the enhancement of UDP-glucuronosyltransferase 2B7 activity by albumin: implications for in vitro-in vivo extrapolation. J Pharmacol Exp Ther. 2007;321(1):137–47. https://doi.org/10.1124/jpet.106.118216.
24. Court MH, Zhang X, Ding X, Yee KK, Hesse LM, Finel M. Quantitative distribution of mRNAs encoding the 19 human UDP-glucuronosyltransferase enzymes in 26 adult and 3 fetal tissues. Xenobiotica. 2012;42(3):266–77. https://doi.org/10.3109/00498254.2011.618954.
25. Harbourt DE, Fallon JK, Ito S, Baba T, Ritter JK, Glish GL, et al. Quantification of human uridine-diphosphate glucuronosyl transferase 1A isoforms in liver, intestine, and kidney using nanobore liquid chromatography–tandem mass spectrometry. Anal Chem. 2012;84(1):98–105. https://doi.org/10.1021/ac201704a.
26. Bhasker CR, McKinnon W, Stone A, Lo AC, Kubota T, Ishizaki T, et al. Genetic polymorphism of UDP-glucuronosyltransferase 2B7 (UGT2B7) at amino acid 268: ethnic diversity of alleles and potential clinical significance. Pharmacogenetics. 2000;10(8):679–85.
27. Kiang TK, Ensom MH, Chang TK. UDP-glucuronosyltransferases and clinical drug–drug interactions. Pharmacol Ther. 2005;106(1):97–132. https://doi.org/10.1016/j.pharmthera.2004.10.013.